Quantitative Comparison of Pyranose Dehydrogenase Action on Diverse Xylooligosaccharides

Johanna Karppi[1], Hongbo Zhao[2], Sun-Li Chong[2,3], Antti E. Koistinen[1], Maija Tenkanen[2] and Emma Master[1,4]*

[1] Department of Bioproducts and Biosystems, Aalto University, Espoo, Finland, [2] Department of Food and Nutrition, University of Helsinki, Helsinki, Finland, [3] State Key Laboratory of Subtropical Silviculture, Zhejiang A&F University, Hangzhou, China, [4] Department of Chemical Engineering and Applied Chemistry, University of Toronto, Toronto, ON, Canada

Pyranose dehydrogenases (PDHs; EC 1.1.99.29; AA3_2) demonstrate ability to oxidize diverse carbohydrates. Previous studies of these enzymes have also uncovered substrate-dependent regioselectivity, along with potential to introduce more than one carbonyl into carbohydrate substrates. Enzymatic oxidation of carbohydrates facilitates their further derivatization or polymerization into bio-based chemicals and materials with higher value; accordingly, PDHs that show activity on xylooligosaccharides could offer a viable approach to extract higher value from hemicelluloses that are typically fragmented during biomass processing. In this study, AbPDH1 from *Agaricus bisporus* and AmPDH1 from *Leucoagaricus meleagris* were tested using linear xylooligosaccharides, along with xylooligosaccharides substituted with either arabinofuranosyl or 4-*O*-(methyl)glucopyranosyluronic acid residues with degree of polymerization of two to five. Reaction products were characterized by HPAEC-PAD to follow substrate depletion, UPLC-MS-ELSD to quantify the multiple oxidation products, and ESI-MS^n to reveal oxidized positions. A versatile method based on product reduction using sodium borodeuteride, and applicable to carbohydrate oxidoreductases in general, was established to facilitate the identification and quantification of oxidized products. AbPDH1 activity toward the tested xylooligosaccharides was generally higher than that measured for AmPDH1. In both cases, activity values decreased with increasing length of the xylooligosaccharide and when using acidic rather than neutral substrates; however, AbPDH1 fully oxidized all linear xylooligosaccharides, and 60–100% of all substituted xylooligosaccharides, after 24 h under the tested reaction conditions. Oxidation of linear xylooligosaccharides mostly led to double oxidized products, whereas single oxidized products dominated in reactions containing substituted xylooligosaccharides. Notably, oxidation of specific secondary hydroxyls vs. the reducing end C-1 depended on both the enzyme and the substrate. For all substrates, however, oxidation by both AbPDH1 and AmPDH1 was clearly restricted to the reducing and non-reducing xylopyranosyl residues,

where increasing the length of the xylooligosaccharide did not lead to detectable oxidation of internal xylopyranosyl substituents. This detailed analysis of AbPDH1 and AmPDH1 action on diverse xylooligosaccharides reveals an opportunity to synthesize bifunctional molecules directly from hemicellulose fragments, and to enrich for specific products through appropriate PDH selection.

INTRODUCTION

Hemicelluloses comprise a diverse group of polysaccharides present in plant cell walls, and are thought to strengthen cell wall structures through interactions with both cellulose and lignin (Ebringerová, 2006; Scheller and Ulvskov, 2010). Xylans are the dominant hemicellulose in cell walls of both grasses and deciduous trees. In deciduous trees, the main xylan is glucuronoxylan, where the β-(1→ 4)-linked D-xylopyranose (Xylp) backbone can be substituted with 4-O-methylated glucopyranosyluronic acid (MeGlcpA); the Xylp backbone can also be acetylated (Ebringerová, 2006; Scheller and Ulvskov, 2010). Arabinoxylans (AXs) are the main xylans in grasses, where the Xylp backbone can be substituted with L-arabinofuranose (Araf). In addition to Araf, arabinoglucuronoxylans found in cell walls of both grasses and coniferous trees, contain glucuronic acid and MeGlcpA substitutions (Scheller and Ulvskov, 2010).

So far, biocatalysts that transform hemicelluloses have mainly been studied and developed to deconstruct corresponding polysaccharides to sugars that can be fermented to fuels and chemicals (Chundawat et al., 2011). These enzymes include glycoside hydrolases (GHs), carbohydrate esterases (CEs), and auxiliary activities (AAs) that are classified by the Carbohydrate-active enzyme (CAZy) database (www.cazy.org) into multiple GH, CE, and AA families (Lombard et al., 2014). Alternatively, enzymatic functionalization of hemicelluloses, including oligosaccharides liberated during lignocellulose processing, opens new possibilities to make high value bioproducts that retain the carbon and energy stored in starting carbohydrate structures.

Carbohydrate oxidoreductases that act on hemicelluloses without cleaving them are attractive targets for further functionalization (Parikka et al., 2012). Among these are AA3 and AA7 FAD-containing oxidoreductases. Briefly, AA7 activity is restricted to the anomeric carbon of carbohydrate substrates (Huang et al., 2005; Vuong et al., 2013); the resulting lactone undergoes spontaneous ring-opening to the carboxylic acid that can be used in polymerization reactions (MacCormick et al., 2018). On the other hand, AA3 oxidoreductases are reported to oxidize the anomeric carbon and secondary hydroxyls to carboxylic acid or ketone functional groups, respectively (Giffhorn et al., 2000; Levasseur et al., 2013; Sützl et al., 2018). Based on phylogenetic analyses, AA3 sequences have been divided into four subfamilies, including activities such as cellobiose dehydrogenase, alcohol oxidase and pyranose oxidase in subfamilies 1, 3, and 4, respectively. Subfamily 2 is the most complex one of these, comprising enzymes with aryl-alcohol oxidase, aryl-alcohol dehydrogenase, glucose oxidase, glucose dehydrogenases, or pyranose dehydrogenase (PDH) activities (Levasseur et al., 2013; Sützl et al., 2018). From these, AA3_2 PDHs have been shown to oxidize several monosaccharides and some oligosaccharides through single or double oxidation and substrate dependent regioselectivity (Peterbauer and Volc, 2010; Rafighi et al., 2018), which increases their attractiveness on oligosaccharide modification.

PDHs have been found in a narrow group of litter-decomposing fungi within the fungal division Basidiomycota (Peterbauer and Volc, 2010). These extracellular enzymes contain two domains, an FAD-binding and substrate-binding domain (Tan et al., 2013). The active site contains two conserved histidines. His512 of AmPDH1 from *Leucoagaricus meleagris* acts as the main base in the first reductive half-reaction and His556 together with Gln392 and Tyr510 take part in substrate interactions that likely influence the observed substrate specific regioselectivity (Graf et al., 2013, 2015; Tan et al., 2013). After the first half-reaction, the reduced flavin is oxidized by an electron acceptor which acts as the second substrate in the reaction. Along with AmPDH1, AbPDH1 from *Agaricus bisporus* are the two most studied PDHs. AbPDH1 and AmPDH1 oxidize D-xylose to 2,3-diketo-D-xylose (Volc et al., 2000; Sedmera et al., 2006) and display slightly higher relative activity toward D-xylose compared to D-glucose (Volc et al., 2000; Sedmera et al., 2006). In addition to D-xylose, AmPDH1 was shown to oxidize xylobiose (X_2) (Sygmund et al., 2008). PDH activity on oligosaccharides with degree of polymerization (DP) greater than two has been tested using cello- and maltooligosaccharides. Those studies confirm that AbPDH1 and AmPDH1 are both active toward cellotetraose and maltotriose (Volc et al., 1997; Peterbauer and Volc, 2010), and that AmPDH1 is also active toward maltooligosaccharides up to maltoheptaose (Tasca et al., 2007; Peterbauer and Volc, 2010; Rafighi et al., 2018). Among the characterized PDHs, AmPDH1 showed highest catalytic efficiency (k_{cat}/K_m) toward D-xylose (Sygmund et al., 2012), whereas AbPDH1 showed highest catalytic efficiency toward cellobiose, maltose and lactose (Gonaus et al., 2016).

PDH action toward xylooligosaccharides common to hardwood and agricultural resources has not been investigated. Herein, AbPDH1 and AmPDH1 were directly compared in terms of activity toward linear and substituted xylooligosaccharides, and ability to oxidize corresponding substrates at more than one position to create a new class of telechelic building blocks. The analysis of corresponding oligosaccharide products is

complicated by the multiple hydroxyl groups that could potentially be oxidized. Moreover, the oxidized products are inherently unstable in water because they can further transform into various end products. For example, oxidation of the anomeric carbon leads to a lactone which spontaneously hydrolyzes to the carboxylic acid in water (Vuong et al., 2013). Furthermore, secondary hydroxyls that are oxidized to ketones and primary hydroxyls that are oxidized to aldehydes, exist primarily as hydrates (geminal diols) in water (Volc et al., 2002; Andberg et al., 2017). In this study, a new analytical method was developed to simplify and clarify the analysis of oxidized xylooligosaccharides utilizing deuterium to label the oxidized position. By following the deuterated residues by HILIC-MS-ELSD and ESI-MS^n, the oxidation positions were identified and the proportion of each reaction product was quantified. Both AbPDH1 and AmPDH1 were shown to oxidize X$_2$, xylotriose (X$_3$) and xylotetraose (X$_4$) with and without Ara$f$ substitution; however, activity toward acidic glucuronoxylooligosaccharides was 10-times lower than with neutral substrates.

MATERIALS AND METHODS

Materials
Below mentioned growth medium chemicals, yeast extract, yeast nitrogen base, and peptone were purchased from Lab M Ltd. (UK). Salts and vitamins were obtained from Sigma-Aldrich or Merck (Germany). Neutral substrates X$_2$, X$_3$, X$_4$, 3^2-α-L-arabinofuranosyl-xylobiose (A^{3}X), 2^3-α-L-arabinofuranosyl-xylotriose (A^{2}XX), 3^3-α-L-arabinofuranosyl-xylotetraose (XA^{3}XX) were purchased from Megazyme (UK). 2^3-(4-O-methyl-α-D-glucuronyl)-xylotriose (U^{4m2}XX) and 2^3-(4-O-methyl-α-D-glucuronyl)-xylotetraose (XU^{4m2}XX) substrates were prepared as in Koutaniemi et al. (2012) by Dr. T. Vuong, University of Toronto and Dr. S. Koutaniemi, University of Helsinki and kindly provided to the study. The commercial laccase from *Trametes versicolor* (Sigma-Aldrich, Germany) was used in oxidation reactions (described below) to recycle 1,4-benzoquinone (BQ; Sigma-Aldrich, Germany) electron acceptor.

PDH Production and Purification
Agaricus bisporus and *Agaricus meleagris* pyranose dehydrogenases (AbPDH1 and AmPDH1; pyranose:acceptor oxidoreductase, EC 1.1.99.29, CAZy family AA3_2) were expressed in *Pichia pastoris* strain KM71H. Codon optimized genes encoding AbPDH1 and AmPDH1 amino acid sequences (AAW92124 and AAW82997, respectively) were obtained as subcloned in pPICZB plasmids with C-terminal 6 x His tag (GenScript, New Jersey, USA). PDHs were produced in eight 2 l shake-flasks each containing 250 ml of medium. Precultures were grown over night in buffered glycerol-complex medium [BMGY; 100 mM potassium phosphate buffer, pH 6.0, 2% (w/v) peptone, 1% (w/v) yeast extract, 1.34% (w/v) yeast nitrogen base, 4 × 10^{-5}% (w/v) biotin, 1% (v/v) glycerol] at 30°C and 220 rpm. Cells were then transferred to methanol-complex medium (BMMY) containing 0.5% (v/v) methanol

instead of glycerol. Methanol was added to 0.5% (v/v) every 24 h and induction was continued 4 d at 25°C and 220 rpm. After the induction, culture supernatants were recovered and filtered, and the secreted recombinant proteins were purified by affinity chromatography; AbPDH1 was further purified by anion exchange and size exclusion (**Figure S2**). Final protein concentrations were measured using the Bradford method (Bio-Rad Laboratories, US); purified proteins were then aliquoted and stored in −80°C.

Initial Activity Measurements
To select the optimal conditions for the xylooligosaccharide oxidation, the activity of AbPDH1 and AmPDH1 was screened at 30°C with 25 mM substrate (D-xylose or D-glucose) and 5 mM BQ in 50 mM sodium acetate, 50 mM ammonium acetate (at pH values 3.0–5.5), and in 50 mM sodium phosphate (at pH values 6.0–7.0) buffers. Reduction of BQ ($\varepsilon_{abs290nm} = 2.24$ mM^{-1} cm^{-1}) in 250 μl reaction was followed at 290 nm; all reactions were performed in triplicate.
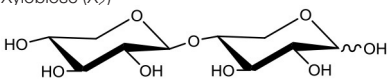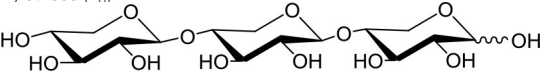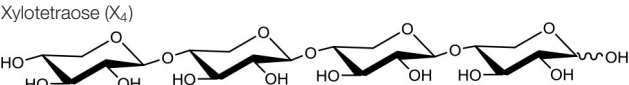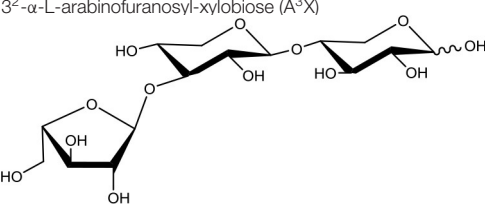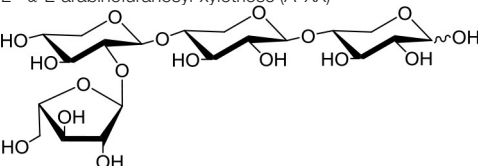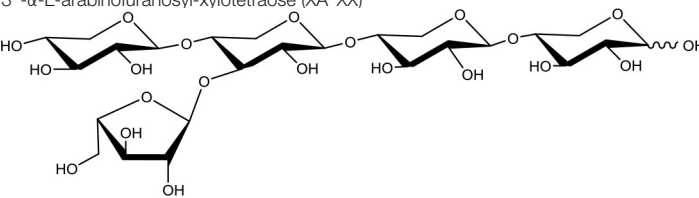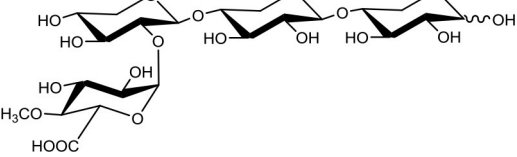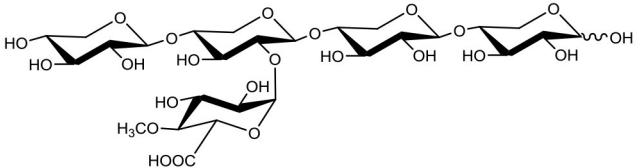
Enzyme loading for PDH conversion of xylooligosaccharides was based on activity units determined in 50 mM ammonium acetate buffer (pH 5.5). PDH activity was measured using 25 mM D-xylose and 5 mM BQ similarly as mentioned above. Laccase activity was measured using 5 mM hydroquinone (HQ, Sigma Aldrich, Germany), and oxidation of HQ ($\varepsilon_{abs249} = 17.25$ mM^{-1} cm^{-1}) in 250 μl reaction was followed at 249 nm.

Initial AbPDH1 and AmPDH1 activity toward xylooligosaccharides was measured using 10 mM neutral or 2 mM of acidic substrates, and 0.2 mM ferrocenium hexafluorophosphate (Fc+, Sigma Aldrich, Germany) as the electron acceptor. Reactions (100 μl) were performed at 30°C in 50 mM sodium phosphate buffer (pH 7.5), and the reduction of the Fc+ ion ($\varepsilon_{abs250nm} = 10.6$ mM^{-1} cm^{-1}) was measured for up to 1 h at 250 nm. All the activity measurements were followed using an Eon plate reader (BioTek, USA).

Enzymatic Conversion of Xylooligosaccharides
Reactions (30–400 μl reaction volume in 1.5 ml Eppendorf tubes) were performed at 30°C for up to 48 h with shaking (500 rpm) in 10 mM ammonium-acetate buffer (pH 5.5) containing 1 mM BQ as the electron acceptor, and 5 mM of neutral xylooligosaccharides or 4 mM of acidic xylooligosaccharides (**Table 1**). Enzyme loadings for reactions containing neutral xylooligosaccharides were 50 mU of AbPDH or AmPDH, and 50 mU of *T. versicolor* laccase. Enzyme loadings for reactions containing acidic xylooligosaccharides were 800 mU of AbPDH1 or AmPDH1, and 800 mU of *T. versicolor* laccase. Time course sampling (25 or 10 μl) for the HPAEC-PAD analyses was done at 1, 4, and 8 h for the neutral substrates and 24 h for acidic substrates. Total reaction time was 24 or 48 h. Oxygen availability was not controlled during the reactions. Reactions were stopped by filtrating the samples through 10 kDa cut off Vivaspin 500 spin columns (Sartorius, Germany) and then kept frozen at −80°C before analysis by High-Performance Anion-Exchange Chromatography Coupled

TABLE 1 | Structures of xylooligosaccharides and oxidation reaction details.

Substrate	Substrate (mM)	PDH (U/ml)	Reaction[a] time (h)
Xylobiose (X$_2$)	5	0.2	Up to 24
Xylotriose (X$_3$)	5	0.2	Up to 24
Xylotetraose (X$_4$)	5	0.2	Up to 24
3^2-α-L-arabinofuranosyl-xylobiose (A^{3}X)	5	0.2	Up to 24
2^3-α-L-arabinofuranosyl-xylotriose (A^{2}XX)	5	0.2	Up to 24
3^3-α-L-arabinofuranosyl-xylotetraose (XA^{3}XX)	5	0.2	Up to 24
2^3-(4-O-methyl-α-D-glucuronyl)-xylotriose (U^{4m2}XX)	4	0.2	Up to 48
	4	2	Up to 24
2^3-(4-O-methyl-α-D-glucuronyl)-xylotetraose (XU^{4m2}XX)	4	0.2	Up to 48
	4	2	Up to 24

[a] All the reactions contained 0.2 U/ml of laccase and 1 mM BQ as electron acceptor.

with Pulsed Electrochemical Detection (HPAEC-PAD) and mass spectrometry as described below.

Quantification of Substrate Depletion by HPAEC-PAD

Products of reactions described above (section *Enzymatic Conversion of Xylooligosaccharides*) were diluted in ultrapure water to 50–100 ppm concentrations depending on the sensitivity of substrate detection by HPAEC-PAD. Substrate depletion over the course of the reaction was followed using a Dionex™-5000^+ system equipped with a Dionex™ CarboPac™ PA1 IC column and corresponding precolumn (Thermo Scientific, USA). The samples were eluted at 1 ml/min with eluent A (0.1 M NaOH) in a linear gradient toward an increasing proportion of eluent B (1 M NaOAc in 0.1 M NaOH). The gradient reached 21.7% B at 20 min after injection, 38% B at 25 min and 100% B at 27 min after which it was kept at 100% for 7 min. Data were analyzed using the Thermo Scientific Dionex Chromeleon 7 Chromatography Data System (version 7.2 SR4, Thermo Fisher Scientific). Corresponding xylooligosaccharides with three known concentrations were used to create a standard curve for each run. Integrated peak areas of the enzyme treated xylooligosaccharides were compared against the corresponding control reactions without the PDH enzyme.

Mass Spectrometric Analysis of Oxidized Products by Direct Infusion

A 5 μl sample from 24 h reactions described above (section *Enzymatic Conversion of Xylooligosaccharides*) was mixed with 5 μl of 10 mg/ml NH_4Cl and 500 μl 50% acetonitrile (ACN) in water. Each sample solution was then introduced into Quadruple Time-of-flight (Q-Tof) mass spectrometry with an ESI source (SYNAPT G2-Si, Waters, MA, USA) at a flow rate of 5 μl/min. The capillary was set to 3 kV; source temperature to 80°C and desolvation temperature to 150°C. The cone gas was 100 l/h and desolvation gas was 600 l/h with nebulizer set at 6.5 bar. The analysis was done in negative mode and the ions were collected in *m/z* range of 50–800. The products of acidic xylooligosaccharides oxidized by 2 U/ml PDH for 24 h were analyzed directly by ESI-Q-Tof-MS without the addition of NH_4Cl.

Identification of Oxidized Positions Through Fragmentation Analysis of Products After NaBD₄ Reduction

The multiple potential oxidations and reactivity of oxidized products in water complicate the interpretation of MS spectra. Therefore, after confirming the production of oxidized xylooligosaccharides by direct infusion mass spectrometry, reaction products were reduced using $NaBD_4$ to facilitate their identification. Specifically, $NaBD_4$ was added to the 24 h reactions described above (section *Enzymatic Conversion of Xylooligosaccharides*) at 3 mol equivalent $NaBD_4$ per mole of substrate in the initial reaction; the resulting solution was then stirred overnight to reduce the carbonyls back to hydroxyls.

After reduction, samples were desalted using Porous Graphitic Carbon (PGC) columns (Hyper carb PGC 50 mg, Thermo Fisher, MA, USA). Briefly, a column was pre-washed with 0.1% trifluoroacetic acid (TFA) 80% ACN and water before loading a sample. The impurities were washed away with Milli Q water and the reaction products were eluted with 50% ACN. The purified samples were then lyophilized, dissolved in 200 μl MilliQ-water, and diluted to 10 μg/ml using 50% ACN, after which ammonium chloride (10 mg/ml) was added to a final concentration of 40 μg /ml. The negative ion MS and MS^n spectra were obtained by direction infusion of the solutions to the Finnigan LXQ Ion Trap (IT) mass spectrometer equipped with ESI source (Thermo Fisher, MA, USA) at a flow rate of 5 μl/min. The parameters were automatically tuned by the instrument based on X_3. The collision energy for fragmentation was optimized based on each substrate.

X_2 and its oxidized products after reduction were not successfully purified by the PGC column. Instead, they were analyzed by Acquity Ultra High Performance Liquid Chromatography (UPLC) coupled to an ESI-Q-Tof mass spectrometer (Waters, MA. USA) as described in **Figure S12**.

Quantification of Oxidized Products by UPLC-ESI-Q-Tof-MS and UPLC Evaporative Light Scattering Detection (ELSD)

The reaction products after $NaBD_4$ reduction and PGC purification were quantified using an Acquity UPLC coupled with ELSD (Waters, MA, USA). A 1.7 μm, 2.1*150 mm Acquity UPLC BEH Amide column (Waters, MA, USA) was used to separate the reaction products. The mobile phases were (A) ACN with 0.1% ammonium hydroxide and (B) 20% ACN with 0.1% ammonium hydroxide. The elution gradient was as follows: from 96% ACN to 50% ACN in 10 min, isocratic (50% ACN) for 2 min, back to 96% ACN in 0.01 min, and 18 min re-equilibrium in initial conditions. The flow was at 250 μl/min with column temperature at 35°C. The ELSD drift tube temperature was set to 40°C and the gain to 200. The nebulizer was set to cooling and pressure to 40 psi. Reaction products were diluted with pure ACN to ~3,000 ng of reaction products per 7 μl of injected sample. External standards were made by reducing and purifying the pure substrates using the PGC column as described in section *Identification of Oxidized Positions Through Fragmentation Analysis of Products After NaBD₄ Reduction*. Standard curves were made by injecting 200–3,750 ng of each reduced substrate for each injection. The Acquity UPLC coupled with ESI-Q-Tof-MS was used to identify the peaks in ELSD chromatogram. The parameters for ESI-Q-Tof were set to the same as mentioned in section *Mass Spectrometric Analysis of Oxidized Products by Direct Infusion*, except that the desolvation temperature was set to 400°C. Quantitative analysis of the reaction products using the UPLC-ELSD and mass spectra collected in section *Identification of Oxidized Positions Through Fragmentation Analysis of Products After NaBD₄ Reduction* was then achieved as described below (section *Quantitative Interpretation of Mass Spectra*).

Quantitative Interpretation of Mass Spectra

Following $NaBD_4$ reduction of oxidized xylooligosaccharides, the same m/z value can be obtained for isotopic non-oxidized xylooligosaccharides and specific oxidized products. For example, the monoisotopic mass of X_3 has an m/z of 452, and the naturally present isotopic chloride, carbon, hydrogen and oxygen generate m/z values of 453 and 454. At the same time, single oxidation of a secondary hydroxyl in X_3 followed by $NaBD_4$ reduction will also generate a peak at m/z 453, and double oxidation of secondary hydroxyls in X_3 followed by $NaBD_4$ reduction will generate a peak at m/z 454 (**Figure S1**). Therefore, the following system of equations (Equations 1–4) was established to calculate the percent of single oxidized and double oxidized products, taking into account the abundance of naturally present isotopic substrate:

Abundance of isotopic m/z for a given reduced oligosaccharide

= abundance of non-oxidized oligosaccharide

+ abundance of single oxidized oligosaccharide

+ abundance of double oxidized oligosaccharide

$$= a + (b - a \times r1 \div 100)$$
$$+ \{ c - a \times r2 \div 100 - (b - a \times r1 \div 100) \times r1 \div 100 \} \quad (1)$$

where a, b, and c are the abundance of m/z values corresponding to non-oxidized, single oxidized, and double oxidized oligosaccharides in reactions following enzymatic oxidation (e.g., m/z 452, 453, and 454, respectively, for X_3); and r1 and r2 are the abundances of corresponding m/z values naturally present the isotopic substrate.

Therefore:

$$\text{Non-oxidation\%} = 100\% - \text{single oxidation\%}$$
$$- \text{double oxidation\%} \quad (2)$$

where:

Single oxidation%

$$= \frac{\text{Abundance of single oxidized oligosaccharide}}{\text{Abundance of isotopic } m/z \text{ for a given reduced oligosaccharide}}$$
$$\times 100\% \quad (3)$$

Double oxidation%

$$= \frac{\text{Abundance of double oxidized oligosaccharide}}{\text{Abundance of isotopic } m/z \text{ for a given reduced oligosaccharide}}$$
$$\times 100\% \quad (4)$$

When an oligosaccharide is oxidized at the reducing end C-1, the reaction product containing the carboxyl acid forms an anionic, deprotonated species. For example, X_3 oxidized at the C-1 position will have an m/z of 429. Herein, the theoretical isotopic distribution of C-1 oxidized oligosaccharides was generated by Masslynx V4.1. When additional oxidations take place at the secondary hydroxyls, the deuterium label would increase the corresponding m/z value by a corresponding number of Daltons.

Therefore, Equations (1)–(4) can be extended by Equations (5)–(8), to calculate the extent of oxidized products with at least one oxidation at the reducing end C-1:

Abundance of isotopic m/z for a given oligosaccharide oxidized at the reducing end C-1

= abundance of C-1 oxidized oligosaccharide

+ abundance of double oxidized oligosaccharide

+ abundance of triple oxidized oligosaccharide

$$= a' + (b' - a' \times r1' \div 100)$$
$$+ \{ c' - a' \times r2' \div 100 - (b' - a' \times r1' \div 100) \times r1' \div 100 \} \quad (5)$$

where a', b', and c' are the abundance of m/z values corresponding to C-1 oxidized, C-1 oxidized + single oxidation at a secondary hydroxyl, and C-1 oxidized + double oxidation at secondary hydroxyls (e.g., m/z 429, 430, and 431, respectively, for X_3); and r1' and r2' are the relative abundance of theoretically generated isotopic oligosaccharide with one oxidation at reducing end C-1.

In this case, the double oxidation consists of one reducing end C-1 oxidation and one secondary hydroxyl oxidation, and a the triple oxidation consists of one reducing end C-1 oxidation and two secondary hydroxyl oxidation.

Therefore:

$$\text{Reducing end C-1 oxidation\%} = 100\% - \text{double oxidation\%}$$
$$- \text{triple oxidation\%} \quad (6)$$

where:

Double oxidation%

$$= \frac{\text{Abundance of double oxidized } X_3}{\substack{\text{Abundance of isotopic m/z for a given} \\ \text{oligosaccharideoxidized at the reducing end C-1}}} \times 100\%$$

$$(7)$$

Triple oxidation%

$$= \frac{\text{Abundance of triple oxidized } X_3}{\substack{\text{Abundance of isotopic m/z for a given oligosaccharide} \\ \text{oxidized at the reducing end C-1}}} \times 100\%$$

$$(8)$$

See **Figure S1** for example calculations.

RESULTS

Initial Rates of PDH Action on Xylooligosaccharides

The yield of recombinantly produced and purified AbPDH1 and AmPDH1 was 1.65 and 11.5 mg/l, respectively, where over 90% purity was reached for both enzymes (**Figure S2**). The activity and pH optima of each PDH was comparable to previous studies

when using glucose as the substrate (**Table S1**). Activity on xylose and xylooligosaccharides was then measured using Fc+ ion as the electron acceptor, given the particular sensitivity of the corresponding assay (Sygmund et al., 2008). Both AbPDH1 and AmPDH1 were active on 10 mM X-X_4 and A^3X; furthermore, AbPDH1 was distinguished by its additional activity on A^2XX and XA^3XX under the conditions used (**Figure 1**).

Activity of both enzymes on xylose (43–45 U/mg; **Figure 1**) were similar to those previously reported for the native AmPDH1 (39 U/mg; Sygmund et al., 2008). Overall, AbPDH1 had higher activities toward X_3, X_4, and A^3X compared to corresponding activity of AmPDH1. Notably, the activity of AbPDH1 toward A^3X was comparable to unsubstituted X_2, and AbPDH1 activity toward A^2XX and XA^3XX was ∼40 and 55% of the corresponding unsubstituted X_3 and X_4 substrates. By contrast, the activity of AmPDH1 on A^3X was only 38% of its activity on X_2 and initial activity values could not be obtained for AmPDH1 oxidation of A^2XX or XA^3XX under these conditions. Similarly, initial activities were not obtained for AbPDH1 and AmPDH1 toward $U^{4m2}XX$ or $XU^{4m2}XX$; however, oxidation of all tested xylooligosaccharides by AbPDH1 and AmPDH1 was observed after reaction optimization and prolonged incubation time, as described below.

Measuring Xylooligosaccharide Conversion by AbPDH1 and AmPDH1

To maximize xylooligosaccharide oxidation by AmPDH1 and AbPDH1, the Fc+ electron acceptor used to measure initial rates was replaced with BQ that can be regenerated using laccase
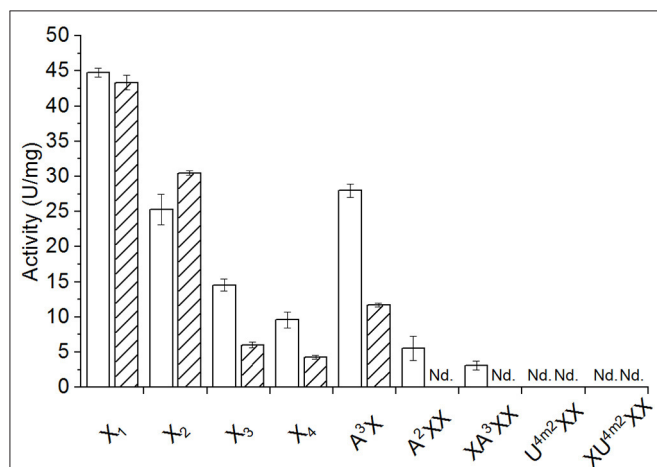

FIGURE 1 | Activity of AbPDH1 (white) and AmPDH1 (with diagonal stripes) on 10 mM of neutral or 2 mM of acidic xylooligosaccharides at pH 7.5 using Fc+ ion as electron acceptor. X_1, xylose; X_2, xylobiose; X_3, xylotriose; X_4, xylotetraose; A^3X, 3^2-α-L-arabinofuranosyl-xylobiose; A^2XX, 2^3-α-L-arabinofuranosyl-xylotriose; XA^3XX, 3^3-α-L-arabinofuranosyl-xylotetraose; $U^{4m2}XX$, 2^3-(4-O-methyl-α-D-glucuronyl)-xylotriose; $XU^{4m2}XX$, 2^3-(4-O-methyl-α-D-glucuronyl)-xylotetraose. Error bars represent standard deviation of three replicate reactions. Reactions with $U^{4m2}XX$ and $XU^{4m2}XX$ were done in duplicates. Nd., no activity detected under these conditions after 24 h.

(Baminger et al., 2001). In an effort to optimize PDH and laccase activities, glucose and xylose oxidation by AmPDH1 and AbPDH1 was tested at pH values ranging from pH 3.0 to 7.0 (**Figure S3**). Based on these analyses, subsequent reactions were performed at pH 5.5. Notably, the addition of laccase clearly increased substrate conversions by both enzymes (**Figure S4**), where up to 85% depletion of xylose (50 mM starting concentration) was reached in 24 h using 5 mM BQ.

Both AbPDH1 and AmPDH1 fully depleted X_2, X_3, and A^3X after 24 h; AbPDH1 also fully depleted X_4 after 24 h (**Figure 2**). With the exception of X_2, substrate depletion was more rapid in reactions containing AbPDH1 than AmPDH1 (**Figure 2**). Differences in substrate conversion were most apparent after 8 h, where X_3 and X_4 conversion by AbPDH1 was 1.2 and 3.9 times higher than by AmPDH1, respectively (**Figures 2B,C**).

When testing AbPDH1 and AmPDH1 activity over 24 h on A^3X, A^2XX, and XA^3XX, minor α-arabinofuranosidase activity was detected in the commercial laccase. Specifically, after 24 h in reactions containing laccase alone, 7.5, 11.5, and 20% of Araf was hydrolyzed from A^3X, A^2XX, and XA^3XX, respectively (**Figures S5–S7**). This reduction of substrate by hydrolysis was taken into account by comparing the substrate depletion in PDH reactions to corresponding control reactions containing laccase alone. Whereas, both AbPDH1 and AmPDH1 were able to fully deplete A^3X by 8 h (**Figure 2D**), A^2XX conversion by AbPDH1 was 1.6 times higher than AmPDH1 after 24 h (**Figure 2E**), and both AbPDH1 and AmPDH1 transformed ∼60% of XA^3XX after 24 h (**Figure 2F**).

When using the same enzyme loading (0.2 U/ml) as for neutral xylooligosaccharides, only AbPDH1 showed clear conversion of both $U^{4m2}XX$ and $XU^{4m2}XX$ (**Figure S8**). Detectable conversion of $U^{4m2}XX$ and $XU^{4m2}XX$ by AmPDH1 was only observed after increasing the enzyme loading 10 times (to 2 U/ml). When comparing AbPDH1 and AmPDH1 after 24 h at the higher enzyme loading, AbPDH1 depleted nearly 100% of both $U^{4m2}XX$ and $XU^{4m2}XX$ whereas substrate depletion by AmPDH1 was ∼30 and 20% for $U^{4m2}XX$ and $XU^{4m2}XX$, respectively (**Figure S8**).

Direct Infusion ESI-Q-Tof Mass Spectrometry Confirms the Formation of Oxidized Xylooligosaccharides

Direct infusion ESI-Q-Tof analyses confirmed that all the tested substrates were oxidized by both AbPDH1 and AmPDH1. The C-1 oxidation products were negatively charged and detected in their anionic form, while neutral oligosaccharides were detected as chlorine adducts. X_2, X_3, X_4, A^3X, A^2XX, XA^3XX gave peaks at mass-to-charge ratios (m/z) 317, 449, 581, 449, 581, and 713, respectively (**Figures S9, S10**). Consistent with the HPAEC-PAD analyses summarized above, low levels of products with a loss of pentose (132 Da) were detected in reactions containing Araf substituted xylooligosaccharides, resulting from α-arabinofuranosidase side activity in the commercial laccase preparation. $U^{4m2}XX$ and $XU^{4m2}XX$ were detected deprotonated [M-H]$^-$ with peaks at m/z 603 and 735, respectively (**Figure S11**).
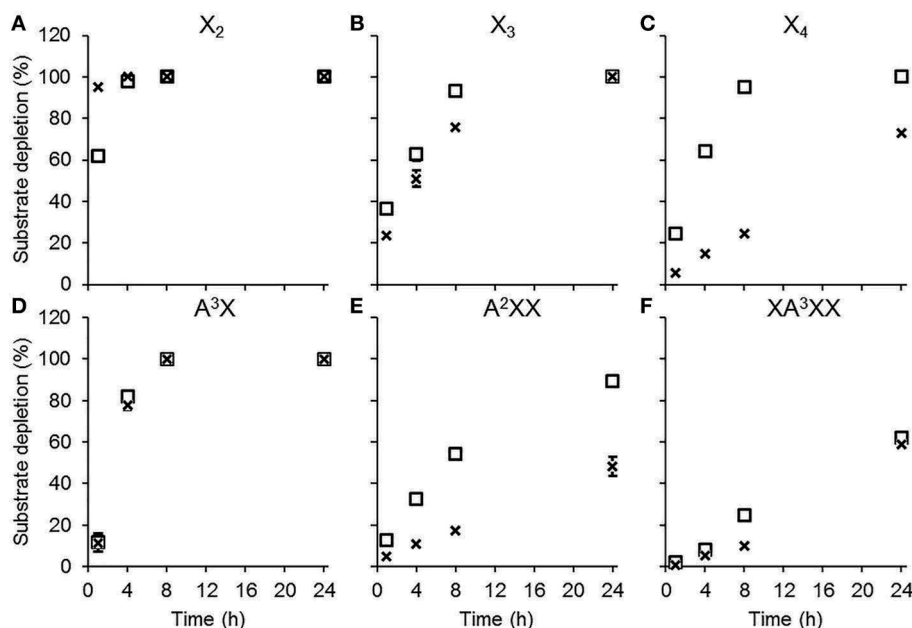
FIGURE 2 | Substrate depletion by AbPDH1 (square) and AmPDH1 (cross) followed by HPAEC-PAD. Substrates: **(A)** xylobiose, X_2, **(B)** xylotriose, X_3, **(C)** xylotetraose, X_4, **(D)** 3^2-α-L-arabinofuranosyl-xylobiose A^3X, **(E)** 2^3-α-L-arabinofuranosyl-xylotriose, A^2XX, and **(F)** 3^3-α-L-arabinofuranosyl-xylotetraose XA^3XX. Depletion of 5 mM substrate using 0.2 U/ml PDHs, 1 mM BQ and 0.2 U/ml laccase was compared to the control reaction containing all reaction components except PDH. Error bars show the data range of duplicate reactions. Error bars are not visible when the data range fits inside the drawn data point.

Both AbPDH1 and AmPDH1 completely consumed X_2 and X_3 after 24 h treatment. By contrast, varying amounts of residual substrate could be detected for X_4 and all substituted xylooligosaccharides. AbPDH1 and AmPDH1 treatment of X_2, A^3X, and XA^3XX resulted in similar MS spectra and thus end products; however, clear differences in product profiles were seen for the other tested substrates. For example, highest peaks following X_3 oxidation by AbPDH1 and AmPDH1 were at m/z 463 and 427, respectively; and highest peaks following X_4 oxidation were at m/z 595/597 and 561, respectively (**Figure S9**). Considering substituted xylooligosaccharides, a peak at m/z 597 represented the highest product peak from A^2XX following 24 h treatment with AbPDH1, whereas the most abundant peak after 24 h AmPDH1 treatment was the non-oxidized A^2XX (m/z 581; **Figure S10**). Consistent with the greater oxidation of neutral xylooligosaccharides by AbPDH1 compared to AmPDH1, the ESI-Q-Tof analyses confirmed significant oxidation of $U^{4m2}XX$ and $XU^{4m2}XX$ by the higher dose of AbPDH1, resulting in peaks at m/z 619 and 751, respectively. By contrast, AmPDH1 oxidized $U^{4m2}XX$ and $XU^{4m2}XX$ to a small percentage (**Figure S11**). Given the higher oxidation of neutral substrates by both enzymes, the corresponding products were analyzed in greater detail.

Qualitative Comparison of Oxidized Xylooligosaccharides Generated by AbPDH1 and AmPDH1

Due to the multiple potential oxidations and reactivity of the oxidized products in water, MS spectra interpretation is challenging. Taking the AbPDH1 oxidized X_3 as an example (**Figure S1C**), the main peak m/z 463 is expectedly representing a

chlorine adduct of a double oxidized product with two carbonyl groups of which the other one has reacted with water to a hydrate (compound A in **Table S2**). Peak m/z 481 is presumably the chorine adduct of the same double oxidized product in which both carbonyls are in the hydrate form. The second most abundant peak m/z 427 is most probably the double oxidized product carrying carboxylic acid group at the reducing end C-1 and one carbonyl group (compound B in **Table S2**) whereas peak m/z 445 can represent the same product in a hydrate form. Mass to charge ratio of 445 can also represent a chlorine adduct of the original double oxidized product with two carbonyl groups. Thus, one compound that is oxidized at two secondary hydroxyls is shown as three peaks in the mass spectrum (compound A in **Table S2**).

To facilitate the interpretation of MS spectra, the oxidized products were treated with $NaBD_4$, and analyzed by ESI-MS after purification. Thus, a PDH oxidation at secondary hydroxyl resulting in a ketone is equivalent to one Dalton difference in mass after $NaBD_4$ reduction compared to substrate (**Figure 3A**). Instead, the oxidation at the reducing end C-1 forms a carboxyl group, which is resistant to $NaBD_4$ reduction (**Figure 3B**). Compared to the chloride adduct of $NaBD_4$ reduced substrate, the oxidation at reducing end C-1 will result in a deprotonated m/z peak that is 23 Da less. Therefore, by counting the Dalton difference between the reduced oxidation products and the reduced original substrates, the number of oxidations occurring in one molecule can be determined.

After $NaBD_4$ reduction, the predominant peak in mass spectra of oxidized X_2 by both PDHs was m/z 322, which is
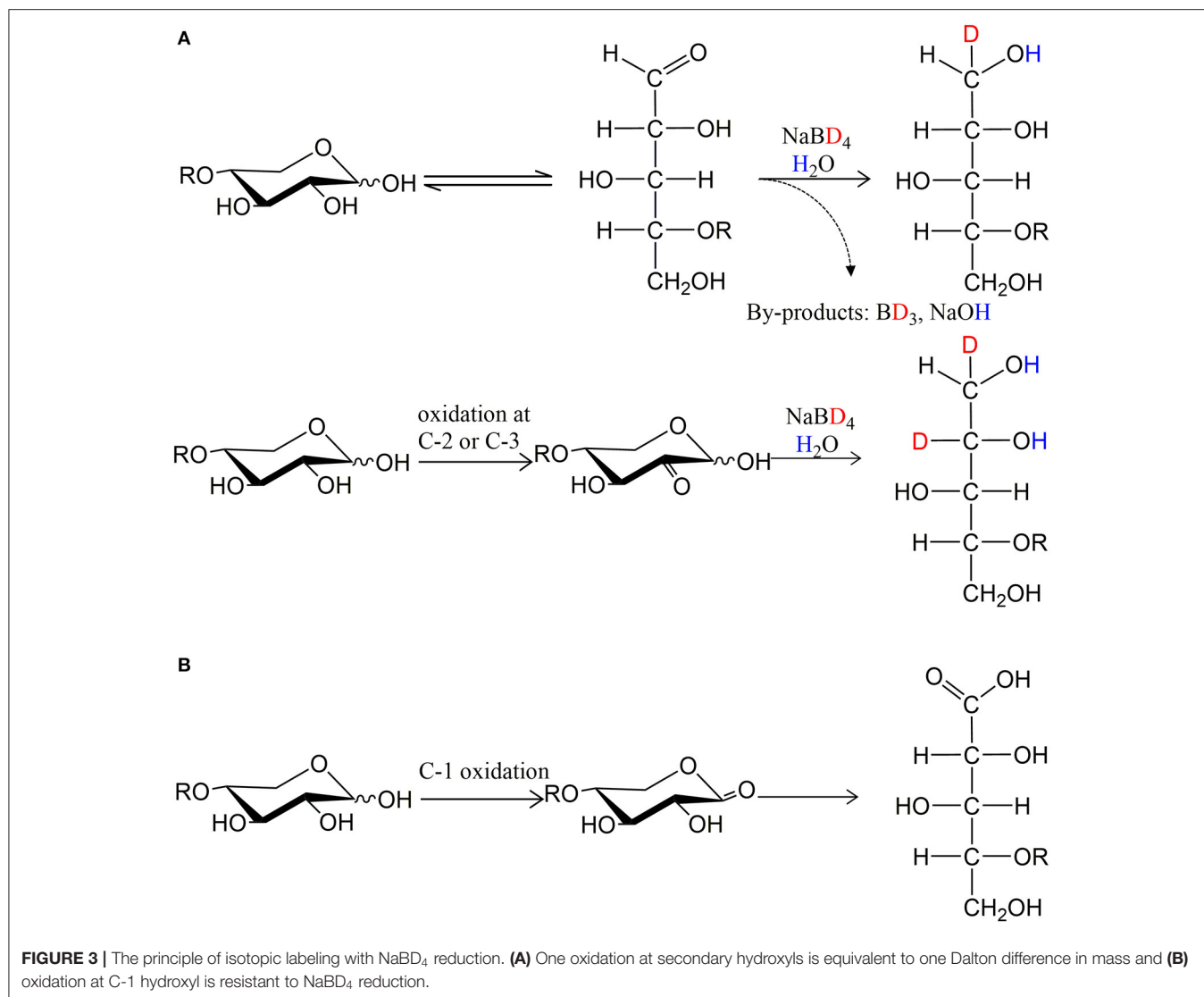
FIGURE 3 | The principle of isotopic labeling with NaBD$_4$ reduction. **(A)** One oxidation at secondary hydroxyls is equivalent to one Dalton difference in mass and **(B)** oxidation at C-1 hydroxyl is resistant to NaBD$_4$ reduction.

2 Da more than the control X$_2$ indicating double oxidation at two secondary hydroxyls (**Figure S12**). The 2 Da increase in mass was also seen for oxidized X$_3$. Oxidation of X$_4$ by both PDHs resulted in single and double oxidized products after 24 h reaction. Notably, Ara$f$ substitution inhibited multiple oxidation of corresponding substrates; A^{3}X and A^{2}XX were mostly single oxidized at a secondary hydroxyl while the XA^{3}XX was still largely non-oxidized by both PDHs after 24 h reaction (**Figure S13**).

In addition to oxidizing secondary hydroxyls, both AbPDH1 and AmPDH1 oxidized the reducing end C-1 of all substrates. Moreover, mass spectra of X$_2$, X$_3$, and X$_4$ products revealed that reducing end C-1 oxidation and secondary hydroxyl oxidations could co-exist in one molecule, resulting in final products with a mass that is 22 Da (reducing end C-1 oxidation + one secondary hydroxyl oxidation) or 21 Da (reducing end C-1 oxidation + two secondary hydroxyls oxidation) less than the control substrate (**Figure S12**).

Direct infusion mass spectrometry after NaBD$_4$ reduction thus confirmed the ability of both AbPDH1 and AmPDH1 to oxidize xylooligosaccharides at multiple positions. Quantification of the reaction products was subsequently important to uncover the specificity of each PDH.

Separate Quantification of Xylooligosaccharides Oxidized at Secondary Hydroxyl Positions and the Reducing End C-1

A two-stage MS-based approach was developed in this study to quantify single and multiply oxidized oligosaccharides, and as well as oxidations at secondary hydroxyls vs. the reducing end C-1 (section *Quantitative Interpretation of Mass Spectra*; see **Figure S1** for example calculation).

Product profiles were first calculated based on mass spectra, where different ionization intensities are obtained for neutral and

acidic products, preventing the direct quantitative comparison of residual substrate products with ketone groups, and acidic products with reducing end C-1 oxidation. As a result, the extent of oxidized secondary hydroxyls and the reducing end C-1 were calculated separately (**Figure 4**). Overall, products with two ketones (i.e., oxidation of two secondary hydroxyls) were dominant for linear xylooligosaccharides. The only exception was AmPDH1 oxidation of X_4, which was only partially oxidized and mainly to a single oxidized product (**Figure 4A**). For all linear xylooligosaccharides treated for 24 h with AbPDH1, products oxidized at the reducing end C-1 were mostly also oxidized at a secondary hydroxyl group (i.e., were double oxidized products, **Figure 4B**). This same pattern was observed for AmPDH1 oxidation of X_3; however, a triple oxidized product (C-1 oxidation + two ketones) represented more than 50% of acidic products generated through AmPDH1 oxidization of X_2. Whereas, oxidation of linear xylooligosaccharides mostly led to double oxidized products, single oxidized products dominated in reactions containing Ara$f$ substituted xylooligosaccharides (**Figures 4A,B**).

Total Comparative Quantification of Oxidized Xylooligosaccharides Generated by AbPDH1 and AmPDH1

Using hydrophilic interaction chromatography (HILIC), acidic and neutral reaction products were successfully separated and identified by MS (**Figures S14, S15**). The acidic products (C-1 oxidation) eluted earlier than the neutral ones and these two classes of products could be quantified after HILIC separation with on-line ELSD using external standards. The ELSD quantification was successfully done for X_3, X_4, A^3X, A^2XX, and XA^3XX products. Due to co-elution with salts, X_2 products could not be quantified. Six reaction species could be quantified: non-oxidized substrate, one oxidation at a secondary hydroxyl, two oxidations at secondary hydroxyls, one oxidation at the reducing end C-1, one oxidation at reducing end C-1 with one oxidation at secondary hydroxyl, and one oxidation at reducing end C-1 with two oxidations at secondary hydroxyls (**Figure 5**).
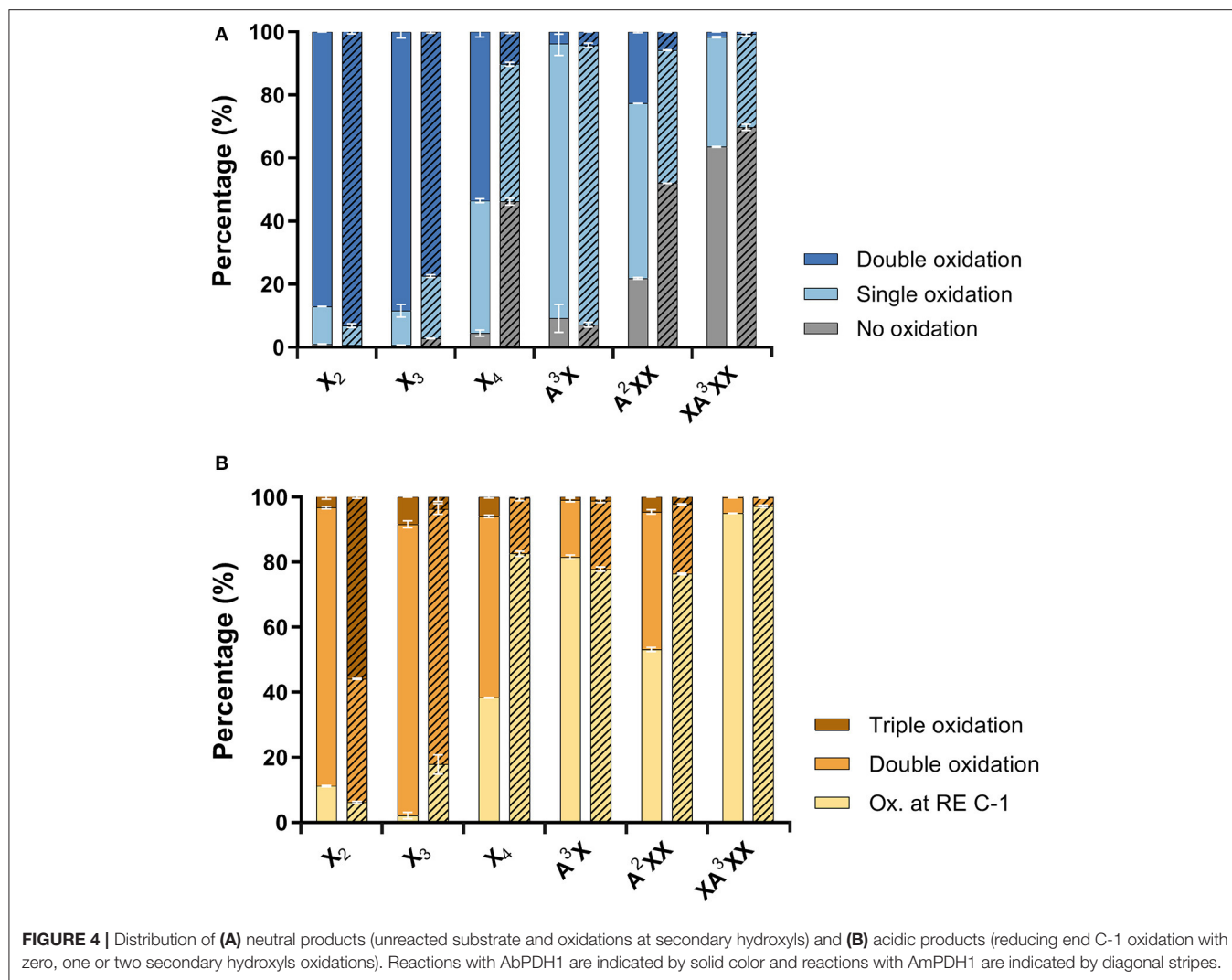
AbPDH1 and AmPDH1 primarily oxidized secondary hydroxyls, and to a lesser extent the anomeric C-1. The main, double oxidized derivative with two ketone groups represented 81 and 56% of X_3 products after 24 h treatment by AbPDH1 and AmPDH1, respectively (**Figure 5**). AbPDH1 also mainly oxidized X_4 at secondary hydroxyls with 38% being single ketone and 48% being double ketone products, whereas the most abundant reaction product after AmPDH1 treatment was C-1 oxidized X_4 (34%). Dominating A^3X products (73–78%) carried single ketone group whereas A^2XX was primary oxidized by AbPDH1 to one (50%) and two (21%) ketone derivatives. After AmPDH1 treatment, 48% of A^2XX remained non-oxidized and 39% of products carried single ketone group. The composition of reaction products from XA^3XX treatments by both PDHs was rather similar, with ∼50% of substrates being non-oxidized after 24 h reaction; ∼25% converted to products with one ketone

group, and 22% were oxidized only at the reducing end C-1 (**Figure 5**).

MS Fragmentation to Determine the Oxidized Residues

The oxidized products after reduction were analyzed using Q-Tof or ion trap by following the deuterium label in the fragment ions. For example, the MS/MS spectrum of reduced X_2 shows the glycosidic linkage cleavage generating Y_1 ion containing the reduced Xyl$p$ residues at m/z 152 (**Figure 6A**). The molecular masses of Y_1 ions carrying 1 Da more than the control sample (**Figures 6B,C**), indicate that one oxidation had taken place at the reducing Xyl$p$ residue by both AbPDH1 and AmPDH1. The mass of precursor ions increased by 2 Da for oxidized samples, thus the other oxidation was at the non-reducing end Xyl$p$ residue. The C-1 oxidized X_2 would have m/z 297 and generate the Y_1 ion at m/z 165 (data not shown). The m/z 298 ion produced the Y_1 ion also at m/z 165 (**Figure 6D**), suggesting one secondary hydroxyl oxidation took place at the non-reducing Xyl$p$ moiety together with the oxidation at reducing end C-1. The Y_1 ion shown in **Figure 6E** increased by 1 Da compared to the compound shown in **Figure 6D**, indicating that AmPDH1 can even generate triple oxidized X_2 with a ketone group at the non-reducing Xyl$p$ residue, a ketone at the reducing Xyl$p$ residue, and a reducing end carboxylic acid.

Following the same procedure as described above for X_2, the oxidized positions for other linear xylooligosaccharides were determined (**Figure 5**; see example MS^n spectra in **Figures S16, S17**). Oxidation by both AbPDH1 and AmPDH1 was clearly restricted to the reducing and non-reducing Xyl$p$ residues. Consistent with quantification using ELSD (section *Separate Quantification of Xylooligosaccharides Oxidized at Secondary Hydroxyl Positions and the Reducing End C-1*), the MS fragmentation confirmed that linear xylooligosaccharides were mostly multi-oxidized by both PDHs, with the exception of X_4 oxidation by AmPDH1 which was dominated by single oxidation. The MS fragmentation further revealed that the oxidation of X_4 by AmPDH1 was localized to the reducing end secondary hydroxyls or reducing end C-1. Surprising, whereas single oxidation of X_4 by both AbPDH1 and AmPDH1 was restricted to the reducing Xyl$p$, single oxidation of X_3 by both PDHs was mainly at the non-reducing end Xyl$p$ secondary hydroxyls (**Figure 5**). Double oxidation by PDHs included products oxidized at (1) secondary hydroxyls of both the reducing and non-reducing Xyl$p$, or (2) the reducing C-1 position and a secondary hydroxyl at the non-reducing end. Increasing the length of the xylooligosaccharide to X_3 and X_4 did not lead to detectable oxidation of internal Xyl$p$ substituents. Interestingly, in addition to the regioselectivity of single and double oxidations, a product of m/z 299 was detected in the AmPDH1 oxidized X_2 after reduction, representing products that were triple oxidized. In this case, it is conceivable that the reducing Xyl$p$ is oxidized at both the reducing end C-1, and a secondary hydroxyl. This was the only detected triple oxidized product.

FIGURE 4 | Distribution of **(A)** neutral products (unreacted substrate and oxidations at secondary hydroxyls) and **(B)** acidic products (reducing end C-1 oxidation with zero, one or two secondary hydroxyls oxidations). Reactions with AbPDH1 are indicated by solid color and reactions with AmPDH1 are indicated by diagonal stripes.

The Ara$f$ substituted substrates were mainly single oxidized or non-oxidized after 24 h treatment. A^{3}X containing α-(1→ 3)-linked Ara$f$ substitution at the non-reducing end Xyl$p$ residue, was single oxidized by both PDHs at the reducing end Xyl$p$ resulting in a ketone group or C-1 oxidized carboxylic acid. A^{2}XX with α-(1→ 2)-linked Ara$f$ substitution was similarly oxidized at the secondary hydroxyl or C-1 of the reducing end Xyl$p$ by both PDHs. Interestingly, in some A^{2}XX products, a second ketone group was detected at the non-reducing end Xyl$p$, which carries the Ara$f$ substituent. Moreover, AmPDH1 showed unique ability to form products with a single ketone group at the non-reducing end Xyl$p$ of A^{2}XX. No clear oxidation of Ara$f$ was detected in any of the samples.

DISCUSSION

AbPDH1 was first isolated over 20 years ago (Volc et al., 1997), and was followed nearly 10 years later by the isolation of AmPDH1 (Sedmera et al., 2006). Since then, AbPDH1 and

AmPDH1 have been biochemically characterized using a broad collection of monosaccharides, heteroglycosides, and selected oligosaccharides, revealing their potential for single and double oxidation of many plant-derived carbohydrates, and motivating their application in biofuel cells and organic syntheses (Giffhorn et al., 2000; Peterbauer and Volc, 2010). Herein, AbPDH1 and AmPDH1 were directly compared in terms of potential to oxidize diverse xylooligosaccharides, both linear and branched, acid and neutral. In particular, we investigated the impact of xylooligosaccharide length and substitution on the extent and position of oxidation by each enzyme. In this way, we evaluated the potential of AbPDH1 and AmPDH1 to serve as catalysts in the synthesis of telechelic building blocks from xylan fragments common to wood and agricultural residues.

Consistent with reported AmPDH1 activity toward X$_2$ (Sygmund et al., 2008) and glucose-containing oligosaccharides (Volc et al., 1997; Tasca et al., 2007; Peterbauer and Volc, 2010; Rafighi et al., 2018) both AbPDH1 and AmPDH1 produced herein oxidized X$_2$ as well as X$_3$ and X$_4$. As observed for PDH activity toward cellooligosaccharides and maltooligosaccharides
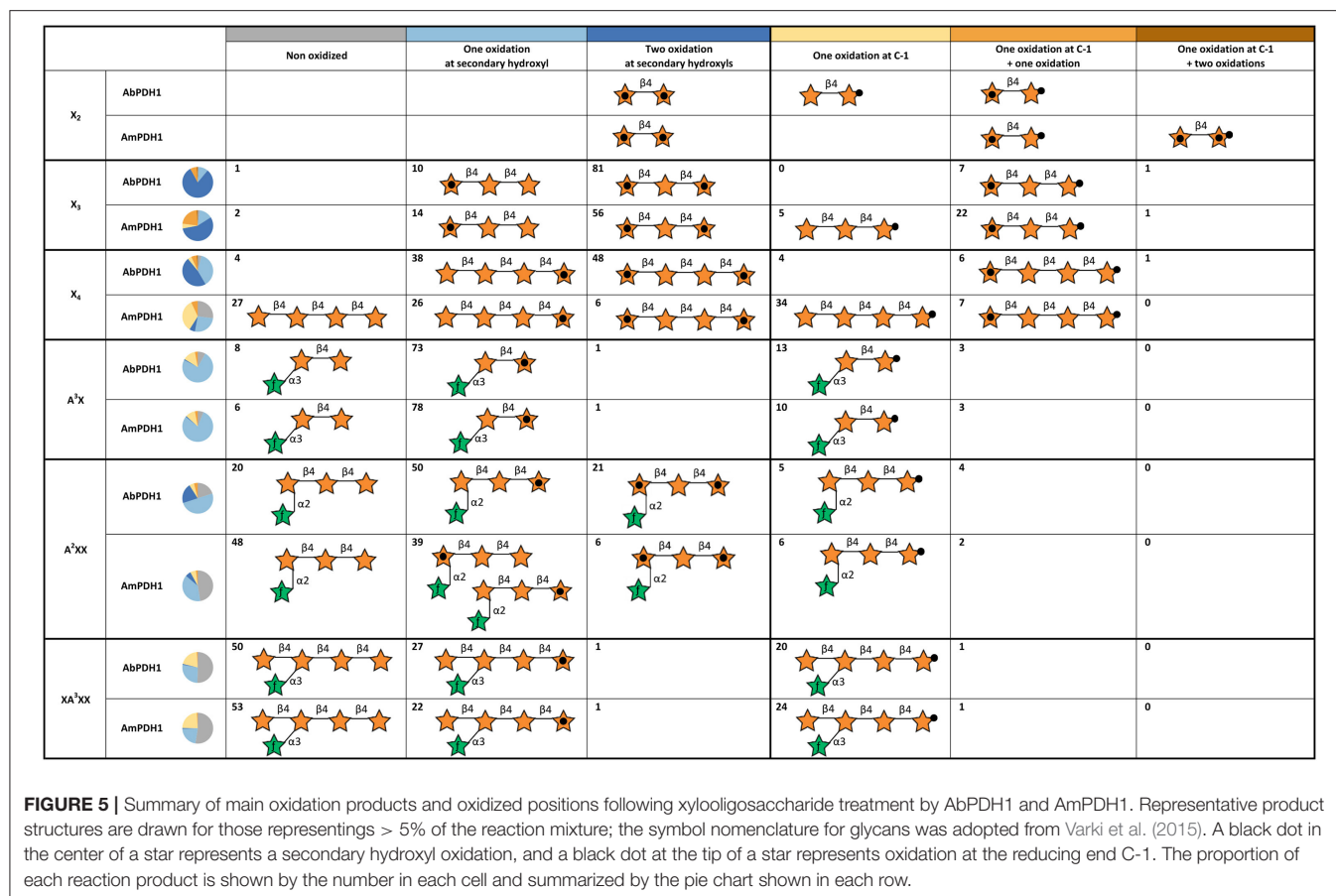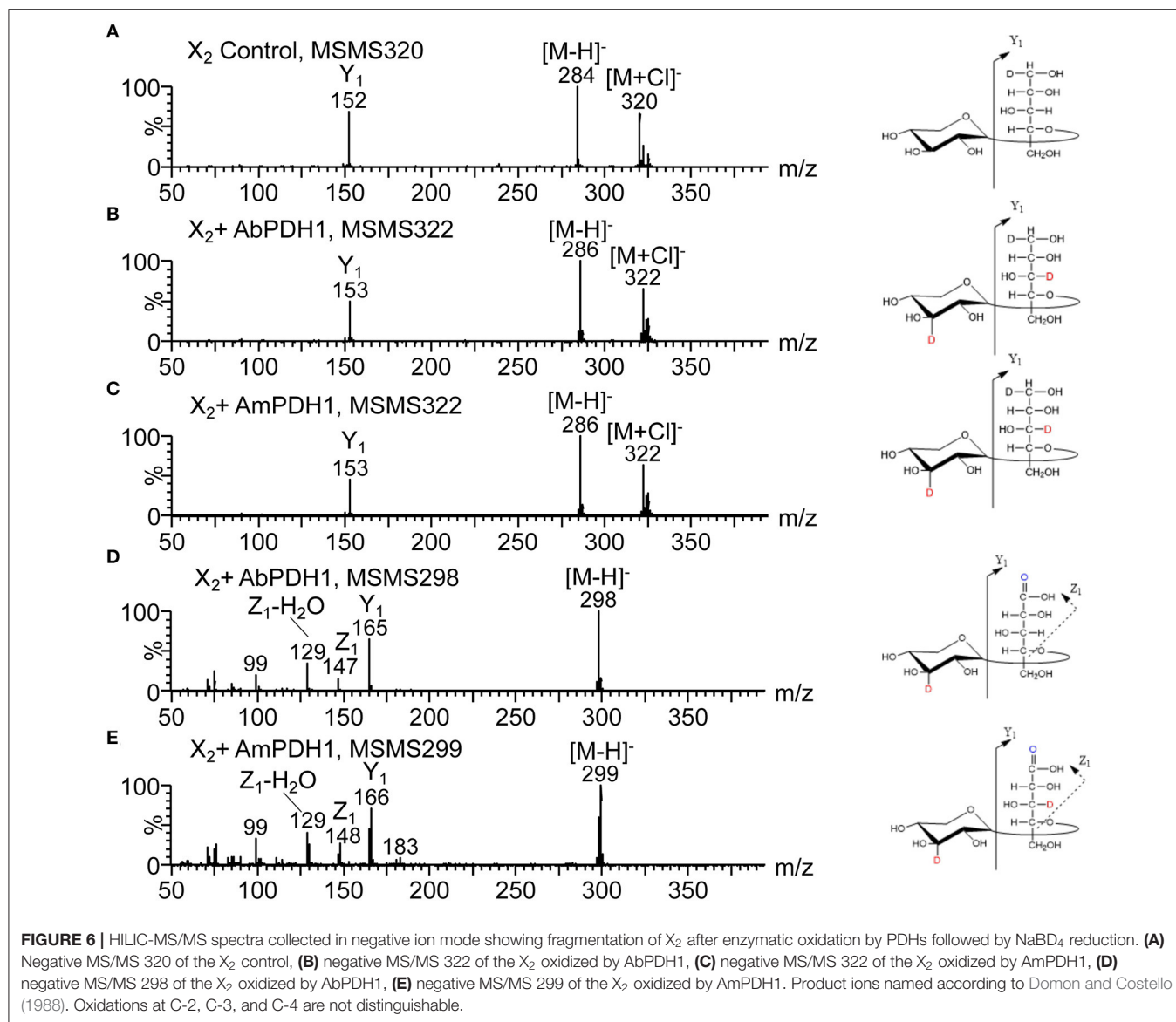
FIGURE 5 | Summary of main oxidation products and oxidized positions following xylooligosaccharide treatment by AbPDH1 and AmPDH1. Representative product structures are drawn for those representings > 5% of the reaction mixture; the symbol nomenclature for glycans was adopted from Varki et al. (2015). A black dot in the center of a star represents a secondary hydroxyl oxidation, and a black dot at the tip of a star represents oxidation at the reducing end C-1. The proportion of each reaction product is shown by the number in each cell and summarized by the pie chart shown in each row.

(Kujawa et al., 2007; Sygmund et al., 2008; Peterbauer and Volc, 2010; Graf et al., 2017), the specific activity (U/mg) of both AbPDH1 and AmPDH1, as well as the rate of the substrate depletion detected with HPAEC-PAD, decreased with increasing degree of polymerization, where the impact of substrate length on activity was greater for AmPDH1 than for AbPDH1. Notably, AmPDH1 depleted X_2 faster than AbPDH1, which is in line with the previous studies, where AmPDH1 shows higher catalytic turnover toward disaccharides, cellobiose, maltose and lactose than AmPDH1 (Sygmund et al., 2008; Gonaus et al., 2016). However, the reverse pattern was observed for longer linear oligosaccharides; AbPDH1 activity toward substituted xylooligosaccharides was also substantially higher than that measured for AmPDH1. In both cases, however, activities toward A^3X were higher than X_3, and activities toward neutral substrates were higher than for the acidic xylooligosaccharides $U^{4m2}XX$ and $XU^{4m2}XX$. The structural basis for these differences in AbPDH1 and AmPDH1 activity toward oligosaccharides awaits a solved structure for AbPDH1 and of enzyme-substrate complexes for this enzyme family. Still, as found in Gonaus et al. (2016), a homology model of AbPDH1 based on the solved structure of AmPDH1 revealed two amino acid deletions in the loop 1 region, differences in the loop 3 region, and substitution of Phe508 in AmPDH1 to the smaller Val505 in AbPDH1. These differences vary the amino acid content in loop regions at the entrance of the

substrate binding pocket, and could impact accessibility of the active site (Gonaus et al., 2016).

When considering the synthesis of telechelic molecules from xylooligosaccharides, it is especially important to evaluate the extent and positions of oxidation in each reaction product. To facilitate this analysis, we established an alternative method for the identification and quantification of oxidized carbohydrates, which utilizes $NaBD_4$ reduction and is solely based on MS and UPLC systems. This method enables fast quantification of formed carbonyl groups as the results are readily interpreted by counting the Dalton difference. In addition, the analysis can be accomplished with reaction products in microgram levels, allowing it to be an attractive technique for characterizing carbohydrate oxidoreductases where enzyme or substrate quantities are limiting. For example, even though specific activity values could not be obtained using the acidic xylooligosaccharides $U^{4m2}XX$ and $XU^{4m2}XX$, the near-complete oxidation of both substrates by AbPDH1 after 24 h was confirmed using this method. Given the higher activity of both AbPDH1 and AmPDH1 on neutral xylooligosaccharides, corresponding product profiles were quantified in more detail. Consistent with activity values, AbPDH1 reached a higher level of double oxidized end products from X_4 and A^2XX compared to AmPDH1. An exception was for X_2, where treatment with AmPDH1 led even to a triple-oxidized product. The ESI-MS^n analyses confirmed

FIGURE 6 | HILIC-MS/MS spectra collected in negative ion mode showing fragmentation of X_2 after enzymatic oxidation by PDHs followed by $NaBD_4$ reduction. **(A)** Negative MS/MS 320 of the X_2 control, **(B)** negative MS/MS 322 of the X_2 oxidized by AbPDH1, **(C)** negative MS/MS 322 of the X_2 oxidized by AmPDH1, **(D)** negative MS/MS 298 of the X_2 oxidized by AbPDH1, **(E)** negative MS/MS 299 of the X_2 oxidized by AmPDH1. Product ions named according to Domon and Costello (1988). Oxidations at C-2, C-3, and C-4 are not distinguishable.

that oxidations were targeted to the reducing and non-reducing ends of all tested xylooligosaccharide substrates. Interestingly, yet unexplained, selectivity was noticed by both enzymes. For example, a single keto group was formed at the non-reducing Xyl*p* residue of X_3, whereas in X_4 a single keto group was found solely at the reducing end Xyl*p*. Also, AmPDH1 produced more C-1 oxidized acidic products from X_3 and X_4 than AbPDH1. As previously reported for activity toward cellobiose, maltose and lactose (Volc et al., 2004; Sygmund et al., 2012; Gonaus et al., 2016), AbPDH1 and AmPDH1 oxidized the anomeric carbon together with secondary hydroxyls of xylooligosaccharides.

Although cross-ring fragmentation was observed in some oxidation products (e.g., with C-1 oxidation), we were not able to identify which secondary hydroxyl was targeted by each enzyme due to proton transfer during the fragmentation (Domon and Costello, 1988). Nevertheless, as reported for glucose-containing

oligosaccharides (Sedmera et al., 2006; Peterbauer and Volc, 2010; Rafighi et al., 2018), the context of the secondary hydroxyls at C-2 and C-3 positions clearly impacted AbPDH1 and AmPDH1 activity toward xylooligosaccharides. Most notably, the alpha-(1→ 3)-linked Ara*f* in A^3X and XA^3XX shifted AbPDH1 and AmPDH1 activity toward the reducing end of both substrates. By contrast, both the reducing and non-reducing ends of A^2XX were oxidized.

In summary, with the newly developed method to identify and quantify oxidized carbohydrates, we successfully determined the degree of oxidation and analyzed the regioselectivity of AbPDH1 and AmPDH1 toward xylooligosaccharides present in wood and agricultural fiber. The widened carbohydrate profile of AbPDH1 and AmPDH1 provides further support for their proposed biological function in evading plant defense mechanisms through reducing plant-derived quinones, or

promoting lignin depolymerization through reducing lignin-derived radicals generated by lignin-active peroxidases and laccases (Peterbauer and Volc, 2010; Sützl et al., 2018; Herzog et al., 2019). Confirming herein that oxidative activity is restricted to the ends of xylooligosaccharides, and that both linear and substituted xylooligosaccharides are accepted, also opens new applications of PDHs that transform underused xylan streams into telechelic molecules primed for polymerization.

DATA AVAILABILITY STATEMENT

The datasets generated for this study are available on request to the corresponding author.

AUTHOR CONTRIBUTIONS

JK, HZ, AK, MT, and EM contributed conception and design of the study. JK, HZ, and AK performed the experiments. JK, HZ, S-LC, and AK analyzed the data. MT and EM contributed reagents, materials, and analysis tools. JK, HZ, MT, and EM wrote the paper. All authors read and approved the submitted version.

FUNDING

ACKNOWLEDGMENTS

SUPPLEMENTARY MATERIAL

The Supplementary Material for this article can be found online at: https://www.frontiersin.org/articles/10.3389/fchem.2020.00011/full#supplementary-material

REFERENCES

Andberg, M., Mollerup, F., Parikka, K., Koutaniemi, S., Boer, H., Juvonen, M., et al. (2017). A novel *Colletotrichum graminicola* raffinose oxidase in the AA5 family. *Appl. Environ. Microbiol.* 83, 1–17. doi: 10.1128/AEM.01383-17

Baminger, U., Ludwig, R., Galhaup, C., Leitner, C., Kulbe, K. D., and Haltrich, D. (2001). Continuous enzymatic regeneration of redox mediators used in biotransformation reactions employing flavoproteins. *J. Mol. Catal.* 11, 541–550. doi: 10.1016/S1381-1177(00)00034-5

Chundawat, S., Beckham, G. T., Himmel, M. E., and Dale, B. E. (2011). Deconstruction of lignocellulosic biomass to fuels and chemicals. *Annu. Rev. Chem. Biomol.* 2, 121–145. doi: 10.1146/annurev-chembioeng-061010-114205

Domon, B., and Costello, C. E. (1988). A systematic nomenclature for carbohydrate fragmentations in FAB-MS/MS spectra of glycoconjugates. *Glycoconj. J.* 5, 397–409. doi: 10.1007/BF01049915

Ebringerová, A. (2006). Structural diversity and application potential of hemicelluloses. *Macromol. Symp.* 232, 1–12. doi: 10.1002/masy.200551401

Giffhorn, F., Köpper, S., Huwig, A., and Freimund, S. (2000). Rare sugars and sugar-based synthons by chemo-enzymatic synthesis. *Enzyme Microb. Technol.* 27, 734–742. doi: 10.1016/S0141-0229(00)00293-3

Gonaus, C., Kittl, R., Sygmund, C., Haltrich, D., and Peterbauer, C. (2016). Transcription analysis of pyranose dehydrogenase from the basidiomycete *Agaricus bisporus* and characterization of the recombinantly expressed enzyme. *Protein Expr. Purif.* 119, 36–44. doi: 10.1016/j.pep.2015.11.003

Graf, M. M., Bren, U., Haltrich, D., and Oostenbrink, C. (2013). Molecular dynamics simulations give insight into d-glucose dioxidation at C2 and C3 by *Agaricus meleagris* pyranose dehydrogenase. *J. Comput. Aided Mol. Des.* 27, 295–304. doi: 10.1007/s10822-013-9645-7

Graf, M. M., Weber, S., Kracher, D., Kittl, R., Sygmund, C., Ludwig, R., et al. (2017). Characterization of three pyranose dehydrogenase isoforms from the litter-decomposing basidiomycete *Leucoagaricus meleagris* (syn. *Agaricus meleagris*). *Appl. Microbiol. Biotechnol.* 101, 2879–2891. doi: 10.1007/s00253-016-8051-1

Graf, M. M. H., Sucharitakul, J., Bren, U., Chu, D. B., Koellensperger, G., Hann, S., et al. (2015). Reaction of pyranose dehydrogenase from *Agaricus meleagris* with its carbohydrate substrates. *FEBS J.* 282, 4218–4241. doi: 10.1111/febs.13417

Herzog, P. L., Sützl, L., Eisenhut, B., Maresch, D., Haltrich, D., Obinger, C., et al. (2019). Versatile oxidase and dehydrogenase activities of bacterial pyranose 2-oxidase facilitate redox cycling with manganese peroxidase *in vitro*. *Appl. Environ. Microbiol.* 85, 1–15. doi: 10.1128/AEM.00390-19

Huang, C. H., Lai, W. L., Lee, M. H., Chen, C. J., Vasella, A., Tsai, Y. C., et al. (2005). Crystal structure of glucooligosaccharide oxidase from *Acremonium strictum*: a novel flavinylation of 6-S-cysteinyl, 8α-N1-histidyl FAD. *J. Biol. Chem.* 280, 38831–38838. doi: 10.1074/jbc.M506078200

Koutaniemi, S., Guillon, F., Tranquet, O., Bouchet, B., Tuomainen, P., Virkki, L., et al. (2012). Substituent-specific antibody against glucuronoxylan reveals close association of glucuronic acid and acetyl substituents and distinct labeling patterns in tree species. *Planta* 236, 739–751. doi: 10.1007/s00425-012-1653-7

Kujawa, M., Volc, J., Halada, P., Sedmera, P., Divne, C., Sygmund, C., et al. (2007). Properties of pyranose dehydrogenase purified from the litter-degrading fungus *Agaricus xanthoderma*. *FEBS J.* 274, 879–894. doi: 10.1111/j.1742-4658.2007.05634.x

Levasseur, A., Drula, E., Lombard, V., Coutinho, P. M., and Henrissat, B. (2013). Expansion of the enzymatic repertoire of the CAZy database to integrate auxiliary redox enzymes. *Biotechnol. Biofuels* 6:41. doi: 10.1186/1754-6834-6-41

Lombard, V., Golaconda Ramulu, H., Drula, E., Coutinho, P. M., and Henrissat, B. (2014). The carbohydrate-active enzymes database (CAZy) in 2013. *Nucleic Acids Res.* 42, D490–D495. doi: 10.1093/nar/gkt1178

MacCormick, B., Vuong, T. V., and Master, E. R. (2018). Chemo-enzymatic Synthesis of Clickable Xylo-oligosaccharide Monomers from Hardwood 4-O-Methylglucuronoxylan. *Biomacromolecules* 19, 521–530. doi: 10.1021/acs.biomac.7b01642

Parikka, K., Leppänen, A. S., Xu, C., Pitkänen, L., and Eronen, P., Österberg, M., et al. (2012). Functional and anionic cellulose-interacting polymers by selective chemo-enzymatic carboxylation of galactose-containing polysaccharides. *Biomacromolecules* 13, 2418–2428. doi: 10.1021/bm300679a

Peterbauer, C. K., and Volc, J. (2010). Pyranose dehydrogenases: biochemical features and perspectives of technological applications. *Appl. Microbiol. Biotechnol.* 85, 837–848. doi: 10.1007/s00253-009-2226-y

Rafighi, P., Bollella, P., Pankratova, G., Peterbauer, C. K., Conghaile, P. Ó., Leech, D., et al. (2018). Substrate preference pattern of *Agaricus meleagris* pyranose dehydrogenase evaluated through bioelectrochemical flow injection amperometry. *ChemElectroChem* 6, 801–809. doi: 10.1002/celc.201801194

Scheller, H. V., and Ulvskov, P. (2010). Hemicelluloses. *Annu. Rev. Plant Biol.* 61, 263–289. doi: 10.1146/annurev-arplant-042809-112315

Sedmera, P., Halada, P., Kubátová, E., Haltrich, D., Prikrylová, V., and Volc, J. (2006). New biotransformations of some reducing sugars to the corresponding (di)dehydro(glycosyl) aldoses or aldonic acids using fungal pyranose dehydrogenase. *J. Mol. Catal.* 41, 32–42. doi: 10.1016/j.molcatb.2006.04.004

Sützl, L., Laurent, C. V. F. P., Abrera, A. T., Schütz, G., Ludwig, R., and Haltrich, D. (2018). Multiplicity of enzymatic functions in the CAZy AA3 family. *Appl. Microbiol. Biotechnol.* 102, 2477–2492. doi: 10.1007/s00253-018-8784-0

Sygmund, C., Gutmann, A., Krondorfer, I., Kujawa, M., Glieder, A., Pscheidt, B., et al. (2012). Simple and efficient expression of *Agaricus meleagris* pyranose dehydrogenase in *Pichia pastoris*. *Appl. Microbiol. Biotechnol.* 94, 695–704. doi: 10.1007/s00253-011-3667-7

Sygmund, C., Kittl, R., Volc, J., Halada, P., Kubátová, E., Haltrich, D., et al. (2008). Characterization of pyranose dehydrogenase from *Agaricus meleagris* and its application in the C-2 specific conversion of D-galactose. *J. Biotechnol.* 133, 334–342. doi: 10.1016/j.jbiotec.2007.10.013

Tan, T. C., Spadiut, O., Wongnate, T., Sucharitakul, J., Krondorfer, I., Sygmund, C., et al. (2013). The 1.6 Å crystal structure of pyranose dehydrogenase from *Agaricus meleagris* rationalizes substrate specificity and reveals a flavin intermediate. *PLoS ONE* 8: e53567. doi: 10.1371/journal.pone.0053567

Tasca, F., Timur, S., Ludwig, R., Haltrich, D., Volc, J., Antiochia, R., et al. (2007). Amperometric biosensors for detection of sugars based on the electrical wiring of different pyranose oxidases and pyranose dehydrogenases with osmium redox polymer on graphite electrodes. *Electroanalysis* 19, 294–302. doi: 10.1002/elan.200603740

Varki, A., Cummings, R. D., Aebi, M., Packer, N. H., Seeberger, P. H., Esko, J. D., et al. (2015). Symbol nomenclature for graphical representations of glycans. *Glycobiology* 25, 1323–1324. doi: 10.1093/glycob/cwv091

Volc, J., Kubátová, E., Wood, D. A., and Daniel, G. (1997). Pyranose 2-dehydrogenase, a novel sugar oxidoreductase from the basidiomycete fungus *Agaricus bisporus*. *Arch. Microbiol.* 167, 119–125. doi: 10.1007/s002300050424

Volc, J., Sedmera, P., Halada, P., Daniel, G., Prikrylová, V., and Haltrich, D. (2002). C-3 oxidation of non-reducing sugars by a fungal pyranose dehydrogenase: spectral characterization. *J. Mol. Catal.* 17, 91–100. doi: 10.1016/S1381-1177(02)00014-0

Volc, J., Sedmera, P., Halada, P., Prikrylová, V., and Haltrich, D. (2000). Double oxidation of D-xylose to D-glycero-pentos-2,3-diulose (2,3-diketo-D-xylose) by pyranose dehydrogenase from the mushroom *Agaricus bisporus*. *Carbohydr. Res.* 329, 219–225. doi: 10.1016/S0008-6215(00)00167-1

Volc, J., Sedmera, P., Kujawa, M., Halada, P., Kubátová, E., and Haltrich, D. (2004). Conversion of lactose to β-D-galactopyranosyl-(1 → 4)-D-arabino-hexos-2-ulose-(2-dehydrolactose) and lactobiono-1,5-lactone by fungal pyranose dehydrogenase. *J. Mol. Catal.* 30, 177–184. doi: 10.1016/j.molcatb.2004.05.006

Vuong, T. V., Vesterinen, A. H., Foumani, M., Juvonen, M., Seppälä, J., Tenkanen, M., et al. (2013). Xylo- and cello-oligosaccharide oxidation by gluco-oligosaccharide oxidase from *Sarocladium strictum* and variants with reduced substrate inhibition. *Biotechnol. Biofuels* 6:148. doi: 10.1186/1754-6834-6-148